Quantification of Flow in a Dynamic Phantom Using ^{81}Rb-^{81m}Kr, and a NaI Detector

John D. Idoine, B. Leonard Holman, Alun G. Jones, Robert J. Schneider,
Kathleen L. Schroeder, and Robert E. Zimmerman

Harvard Medical School and
Peter Bent Brigham Hospital, Boston, Massachusetts

Blood flow can be measured by monitoring the count rate of Krypton-81m after its parent, Rubidium-81 (a potassium analogue), has been deposited in the tissue. The steady-state Kr-81m count rate reflects both production by decay of Rb-81 and washout due to blood flow. Its use is theoretically superior to that of Xenon-133 for quantification of blood flow (cc/min per 100 gm) since: (1) multiple flow measurements can be obtained from a single arterial injection, (2) flow-dependent changes in the count rate of Kr-81m provide a steady-state measure of specific flow, and (3) errors due to uptake in fat are eliminated. The count rate of Kr-81m was measured as a function of flow in a dynamic phantom with a NaI crystal, using both pure cyclotron-produced Rb-81 and commercially available samples with as much as 25% contamination from Rb-82m. The phantom was calibrated by measuring the flow-rate constants with Xe-133. No significant difference was found between the flow-rate constants measured with three pure samples of Rb-81 and those measured with three contaminated samples. The ratio of the zero-flow Kr-81m count rate to the rate observed in the presence of flow showed excellent correlation with calibrated flow over a range of rate constants from 0 to 0.02 sec^{-1}. This study suggests that regional specific flow can be measured in vivo with currently available NaI detecting systems after the intra-arterial injection of Rb-81.

J Nucl Med 18: 570–578, 1977

Quantitative estimates of regional myocardial perfusion have been obtained following the injection of an inert radioactive gas into a coronary artery. Xenon-133, the most frequently used radiotracer for this purpose *(1,2)*, suffers from a number of attendant problems that affect the accuracy of the blood-flow measurement. For example, the high solubility of xenon in fat results in preferential uptake in, and slow washout from, adipose tissues. The necessity of injecting xenon just before each measurement limits the interventions that may be studied. Finally, the recirculation of xenon may introduce a systematic error into the observed washout.

Jones and Matthews *(3)* proposed an alternative technique for measuring tissue perfusion based on

flow-dependent changes in the observed count rate of Kr-81m when its parent, Rb-81 (a potassium analogue), is incorporated in the tissue. Krypton-81m is an inert gas whose clearance from the myocardium is dependent on blood flow. The steady-state Kr-81m count rate reflects both its production (by decay of Rb-81) and washout due to blood flow. Thus, as blood flow increases, the Kr-81m count rate decreases. These characteristics form the basis for potential quantification of blood flow. This variation

of the inert-gas washout technique is potentially superior to the Xe-133 technique because (A) errors due to preferential uptake in fat would be eliminated since Rb-81 is distributed proportional to blood flow; (B) multiple measurements could be made in various projections and with various interventions after a single arterial injection, taking advantage of the more uniform distribution of radiotracer obtained at rest; (C) it would provide a steady-state measure of flow permitting long observation times and correspondingly small statistical uncertainties; and (D) errors due to recirculation would be reduced by the 13-sec half-life of Kr-81m.

Jones and Matthews felt, however, that successful application of the method would require a high-resolution, solid-state detector in order to separate the Kr-81m photopeak from the underlying Compton continuum due to higher-energy photons. Phantom studies with a Ge(Li) detector and cyclotron-produced Rb-81 yielded accurate flow measurements (3), and localization of Rb-81 labeled blood cells in the spleen allowed measurement of blood flow to that organ, again with a Ge(Li) detector (4). However, such detectors are currently impractical for regional flow measurements. Harper et al. (5) used ^{81}Rb–^{81m}Kr to assess myocardial blood flow following an intravenous injection, but concluded that measurements obtained with an Anger camera were not sufficiently precise for clinical application. Several investigators (6–10) have used Kr-81m infusions from an ^{81}Rb–^{81m}Kr generator to visualize relative perfusion, but this technique affords no quantitative estimate of blood flow.

In this study, we measured flow with a NaI detector in a dynamic phantom using both pure cyclotron-produced ^{81}Rb–^{81m}Kr and commercially available samples* with up to 25% contamination with Rb-82m.

THEORY

The ^{81}Rb–^{81m}Kr method takes advantage of the different chemical properties of the parent and daughter. The decay of Rb-81 (11–13) is shown in Fig. 1. The final product, Kr-81, is stable for the purposes of this study ($T_{1/2}$ = 2.1 × 10^5 years). Rubidium-81 is a neutron-deficient nuclide that decays by positron emission and electron capture with a half-life of 4.58 hr. Photons are emitted at 446 keV (0.232 prompt gamma rays from excited Kr-81 per disintegration of Rb-81) and 511 keV (0.615 photons per disintegration of Rb-81) from positron annihilation. Its daughter, Kr-81m, decays by isomeric transition with a half-life of 13 sec, emitting a photon at 190 keV (0.638 photons per disintegration of Rb-81). These gamma-ray intensities
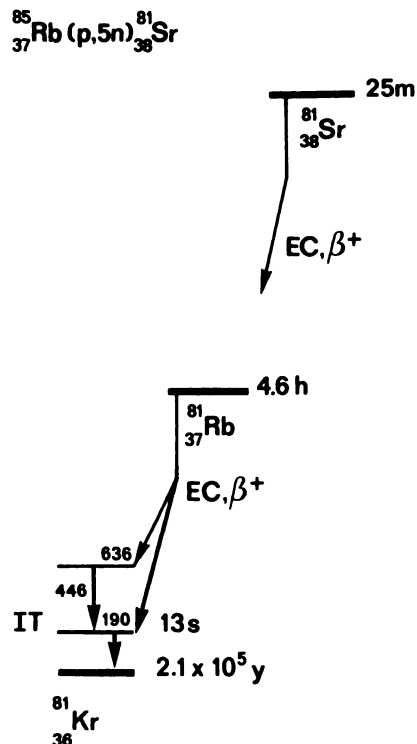

$^{85}_{37}$Rb (p,5n)$^{81}_{38}$Sr

FIG. 1. Simplified decay scheme for chain ^{81}Sr→^{81}Rb→^{81}Kr.

(11) include the attrition of gamma photons due to internal conversion. The major contaminant in commercial samples is Rb-82m (6.4 hr) which produces several high-energy photons (511–1475 keV).

For any parent–daughter system, the number of atoms of the daughter that are present at time t is given by

$$N_2(t) = \left(\frac{k_1}{k_2 - k_1}\right) N_1^\circ (e^{-k_1 t} - e^{-k_2 t})$$
$$+ N_2^\circ e^{-k_2 t}, \quad (1)$$

where the subscripts 1 and 2 refer to parent and daughter, respectively. Here k_i are the decay constants and N_i° are the initial numbers of atoms present. The term $N_2^\circ e^{-k_2 t}$ represents the decay of daughter atoms present at t = 0, and the remainder represents the production and decay of daughter atoms arising from decay of the parent. For the ^{81}Rb–^{81m}Kr system the limiting case of secular equilibrium ($k_2 \gg k_1$) is a useful approximation since $k_2 = 1268 k_1$. Then

$$N_2(t) = \left(\frac{k_1}{k_2}\right) N_1^\circ e^{-k_1 t} \quad (2a)$$

and since $N_1^\circ e^{-k_1 t}$ is the number of parent atoms present at time t,

$$k_1 N_1 = k_2 N_2. \quad (2b)$$

If C_i denotes the *measured* count rate of the ith nuclide in counts/minute, and if d_i is the efficiency of the detection system for the ith nuclide, then

$$C_i = d_i k_i N_i. \qquad (3)$$

The system quickly reaches equilibrium and the count rates for Rb-81 and Kr-81m are equal for equal detection efficiencies.

Consider the effect of flow on the observed count rates. The parent, Rb-81, is a potassium analogue that becomes temporarily incorporated in the myocardial tissue. Thus, after injection into a coronary artery, Rb-81 is distributed throughout the region perfused by that artery; once deposited, its count rate does not vary with changes in flow. The daughter, Kr-81m, however, is an inert gas whose regional clearance from the myocardium is dependent on blood flow. Some Kr-81m atoms will be swept from the detector's field of view before they decay. Thus, the Kr-81m count rate (C_2) will be reduced by those disintegrations that occur outside the field of view.

In the case of monoexponential washout of the Kr-81m atoms at a rate given by the flow-rate constant k_f, the total effective rate constant for the elimination of Kr-81m atoms is

$$k_{eff} = k_2 + k_f. \qquad (4)$$

Replacing k_2 and N_2 in Eq. (2b) by k_{eff} and N_2^{eff} yields

$$N_2^{eff} = \left(\frac{k_1}{k_2 + k_f}\right) N_1. \qquad (5)$$

The number of Kr-81m atoms (N_2^{eff}) that are effectively available for decay and detection is thus reduced as the flow-rate constant (k_f) increases. The observed count rate from Kr-81m will be a function of flow given by analogy with Eq. 3 as

$$C_2 = d_2 k_2 N_2^{eff};$$

and from Eq. 5

$$C_2 = d_2 k_2 \left(\frac{k_1}{k_2 + k_f}\right) N_1 = d_2 k_1 N_1 \left(1 + \frac{k_f}{k_2}\right)^{-1}$$

or

$$\frac{C_2^0}{C_2} = 1 + \frac{k_f}{k_2}, \qquad (6)$$

where $C_2^0 = d_2 k_1 N_1$ is the count rate in the absence of flow. Equation 6 provides the theoretical basis for measuring flow with ^{81}Rb–^{81m}Kr. The rate constant for physical decay (k_2) is known and the Kr-81m count rates, with and without flow, are measured.

For any particular photopeak in a complex spectrum, the distribution of counts may be approximated by the expression
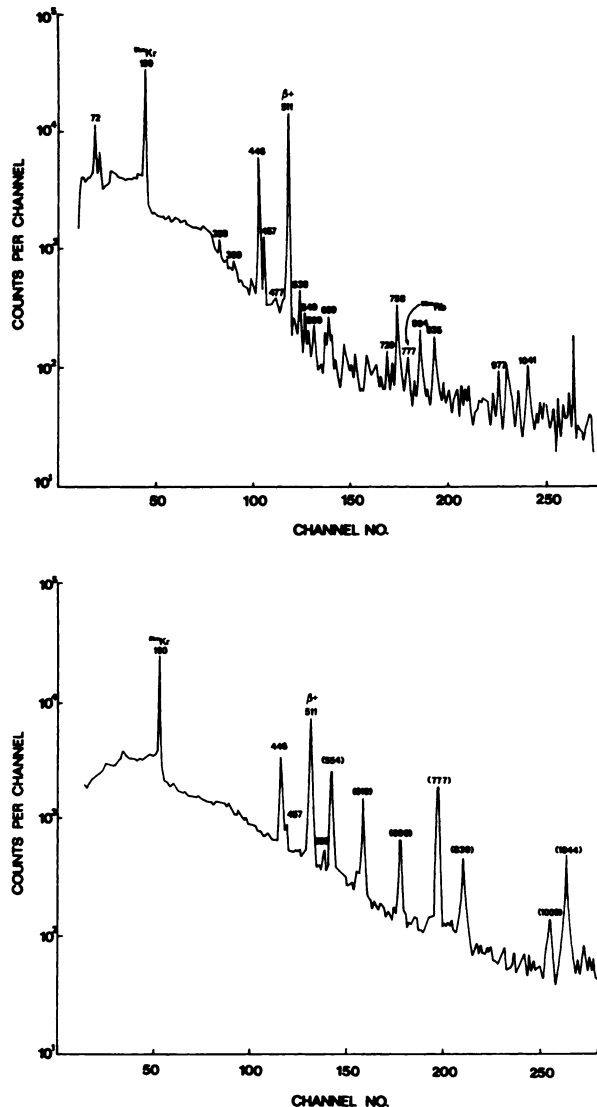

FIG. 2. Ge(Li) spectra of (A, top) pure RB-81 produced by reaction ^{85}Rb(p,5n)^{81}Sr and decay of Sr-81 to Rb-81, (B, bottom) commercially produced Rb-81. Energies in keV, those shown in parentheses are due to contamination with Rb-82m.

$$S(H) = S_0 \exp\left[\frac{-(H - \bar{H})^2}{2\sigma^2}\right] + (BH + D),$$

where the Gaussian term of standard deviation σ represents the distribution of pulse heights (H) about the mean $(\bar{H})$, and the linear term $(BH + D)$ represents the contribution from the Compton continuum due to higher-energy photons. Thus, the area under the Kr-81m photopeak at 190 keV may be approximated by a sum over pulse heights of the total counts less the Compton contribution

$$C_2 = \sum_{\bar{H}-\Delta H}^{\bar{H}+\Delta H} [S(H) - (BH + D)]. \qquad (7)$$

In practice it is convenient to normalize the observed Kr-81m count rate to some portion of the

572

energy spectrum that does not change with flow. The peak at 511 keV due to Rb-81 and the contaminant Rb-82m may be used for this purpose. Normalization eliminates the geometric factor from the detection efficiency, so that measurements in various projections are independent of counting geometry. In particular, errors arising from differences in counting geometry between the zero-flow measurement and the actual distribution of nuclides in the myocardium are avoided. The zero-flow measurement must, however, simulate the correct tissue depth since the observed count rates depend on the transmission through this tissue. Normalization also corrects for changes in the Kr-81m count rate due to the slow washout of Rb-81 from the myocardium. For example, the half-time for the washout of radio-potassium, an analogue of rubidium, is 90 min (14).

METHODS

Production of Rb-81. The production of pure Rb-81 at the Harvard Cyclotron by the reaction $^{85}Rb(p,5n)^{81}Sr$ and decay of Sr-81 to Rb-81 has been described recently (15). Powdered RbCl targets, wrapped in aluminum foil, were irradiated for 15 min at the 70-MeV radius of the cyclotron. The purification of Rb-81 from the RbCl target utilized a separation technique similar to that previously described for other rubidium and strontium isotopes (16). Carrier-free Rb-81 of high radionuclide purity was obtained by a two-step separation with a neutral Al_2O_3 column following irradiation of the RbCl target. The predominant nuclear species after bombardment were Rb-81 (4.58 hr), Rb-82m (6.4 hr), Rb-84m (20.4 min), Sr-81 (25 min), Sr-83 (32.4 hr), and Sr-85m (68 min). The initial separation removed all rubidium isotopes from the column, sacrificing that part of the Rb-81 yield due to the direct reaction $^{85}Rb(p,p4n)^{81}Rb$ but allowing the subsequent buildup of pure Rb-81 from the decay of Sr-81 (Fig. 1). Rubidium-81 was then eluted from the strontium isotopes remaining on the column.

The column consisted of a plastic disposable syringe (11 mm diam. $\times$ 84 mm) fitted at the lower end with a polyethylene disk ($\frac{1}{16}$ in. thick, 25 μ porosity) on which was placed a 2-gm layer of alumina. The elution was regulated by a peristaltic pump connecting the target solution and the buffered eluant to the column. The column was initially equilibrated with the NaOH eluant buffered with 0.01 M sodium acetate for 10 min to obtain a constant pH of 8.6–8.7. Tracer studies showed that this pH range provided optimal retention of carrier-free strontium on the alumina column, while rubidium was eluted. In the first separation, the target was dissolved in 5–6 ml of the buffered eluant, loaded onto the col-

umn at a rate of 1.5 ml/min, and washed with the buffered eluant to remove all rubidium isotopes. The elution of rubidium was essentially complete after 10 min. The Sr-81 left on the column was allowed to decay, with the maximum yield of Rb-81 occurring 90 min (3.6 half-lives) after isolation of the Sr-81. At this time, the Rb-81 was eluted from the remaining strontium isotopes in essentially pure form (less than 1% contamination from other rubidium species). Yields for 15-min bombardments with an estimated beam current of 1 μA have been about 150 μCi of separated Rb-81 per gram of target material. Figure 2A shows a Ge(Li) spectrum of a sample of Rb-81 obtained by this procedure. All the lines were identified with those of Rb-81 as described by Waters (13). By contrast, a spectrum of commercially obtained Rb-81 is shown in Fig. 2B. Most of the higher-energy lines are masked by the large amount of Rb-82m present (22% for this sample).

The phantom. A phantom (Fig. 3) was designed to simulate the behavior of the $^{81}Rb-^{81m}Kr$ combination in the myocardium after injection into a coronary artery. The phantom consisted of a plexiglass chamber, partially filled with water, through which air could be bubbled at a controlled flow rate. When a sample of $^{81}Rb-^{81m}Kr$ was injected into the phantom, the Rb-81 ions remained in solution while the Kr-81m quickly established an equilibrium concentration in the air volume and was washed out by air flowing through the phantom. The phantom was calibrated by monitoring the washout of Xe-133 at various flow rates.

Let A(t) and W(t) be the instantaneous concentrations of inert gas (Kr-81m or Xe-133) in the phantom's air volume (V_a) and water volume (V_w), respectively. If the washout process is not limited by diffusion of inert gas from the water into the air,
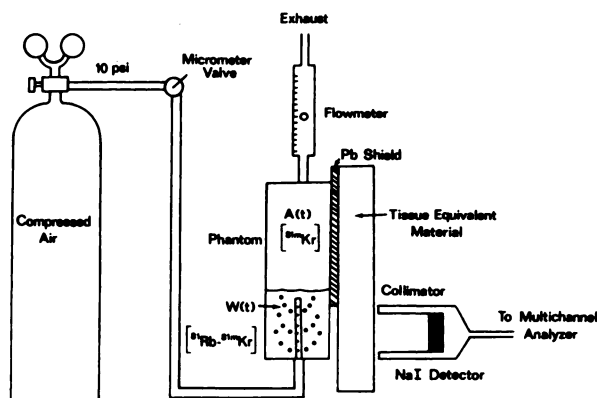

FIG. 3. Dynamic phantom used to measure Kr-81m count rate as function of flow.

then the concentration ratio will be maintained equal to the water:air partition coefficient (λ) of the gas. That is,

$$\frac{W(t)}{A(t)} = \lambda, \qquad (8)$$

where the partition coefficient (λ) remains constant as long as the temperature is constant and the concentrations do not approach saturation. The total activity (Q) in both compartments at any time is then

$$Q(t) = V_w W(t) + V_a A(t)$$
$$= W(t) \left[V_w + \frac{V_a}{\lambda} \right]. \qquad (9)$$

The activity removed from the phantom during an interval of time (dt) due to a flow (F) is

$$dQ(t) = -A(t)Fdt = dW(t) \left[V_w + \frac{V_a}{\lambda} \right], \qquad (10)$$

assuming complete and instantaneous mixing in the air volume. Combining Eqs. 8 and 10 yields

$$\frac{dW(t)}{dt} = \frac{-W(t)F}{(\lambda V_w + V_a)}$$

and

$$W(t) = W_o \exp[(-Ft)(\lambda V_w + V_a)^{-1}], \qquad (11)$$

where W_o is the initial concentration.

Equation 11 describes the monoexponential washout of activity from the water volume in the phantom at a rate given by

$$k_f = \frac{F}{(\lambda V_w + V_a)}. \qquad (12)$$

The phantom was calibrated by measuring k_f as a function of flow for washout of Xe-133. A 3-in. NaI detector was used to monitor the washout of Xe-133 from the water. The rate constants (k_f) were determined by fitting an unweighted least-squares regression line to the logarithm of the resulting time–activity curves. Because the ratio of volumes for the phantom was $V_a/V_w = 1.6$, the washout rates (k_f) were relatively insensitive to the differences in the partition coefficients (17–19) of xenon ($\lambda = 0.13$) and krypton ($\lambda = 0.06$) in water at 25°C. The rate constants (k_f) for the washout of Kr-81m were assumed to be equal to those measured with Xe-133, after correction for the difference in partition coefficients of the two gases in water according to Eq. 12. The advantage of using the flow of air through liquid to create the washout (as opposed to liquid through liquid) is that the vigorous mixing of the air bubbles reduces the distances through which the inert gas (Kr-81m or Xe-133) must diffuse. This minimizes any calibration errors arising due to differences in

the diffusivities of krypton and xenon, and allows the phantom to produce monoexponential washouts over a wide range of flow rates.

Flow through the phantom was set by adjusting the micrometric capillary valve† until the desired flow was obtained. The phantom chamber and the flowmeter operated near atmospheric pressure, independent of pressure changes elsewhere in the system, thus enhancing both the reproducibility and stability of the washout. The resulting reproducibility, based on the washout of Xe-133 from the phantom, was ±2% over the useful range of the flowmeter from 100 to 1900 ml/min. After initial adjustment, no statistically significant change in phantom flow was observed over 30 min of continuous operation. Thus, no variation in washout rate occurred during the acquisition of any ^{81}Rb–^{81m}Kr spectrum (5–10 min). To facilitate the diffusion of inert gas into the air volume, the phantom manifold was designed to provide vigorous bubbling. The monoexponential character of the Xe-133 washout was demonstrated by the linearity of the log W(t) washout curves. The correlation coefficient was greater than 0.99 in each case, while the uncertainty in the slope was less than 1%.

The ratio of Kr-81m count rates (C_2^o/C_2) was measured in the dynamic phantom as a function of flow for rate constants (k_f) in the range 0 to 0.04 sec^{-1}. This range corresponds to the rate constants that could be observed with blood flow of 0–240 cc/min per 100 gm, assuming a blood:tissue partition coefficient of 1.0 for Kr-81m (20) and unit-density tissue. Each measurement consisted of the acquisition of a complete (0–1 MeV) energy spectrum of the ^{81}Rb–^{81m}Kr combination in the water
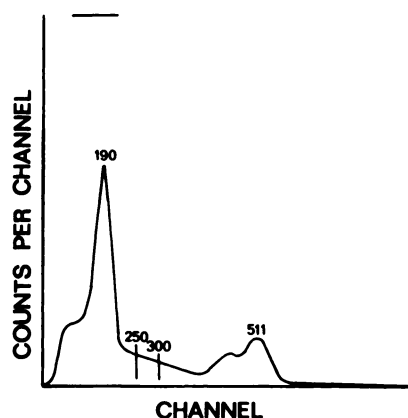

FIG. 4. NaI spectrum of pure Rb-81 measured in dynamic phantom at flow rate comparable to 232 cc/min per 100 gm. Line above Kr-81m peak at 190 keV is height observed in absence of flow. Crossover correction was based on linear extrapolation of segment between 250 and 300 keV.

574

volume. A typical NaI spectrum obtained in the flow measurements is shown in Fig. 4.

The Compton correction was based on a linear extrapolation of the indicated segment of the energy spectrum. A linear least-squares fit to the Compton continuum from 250 to 300 keV generated the parameters B and D, which were then used to calculate the Kr-81m count rate using Eq. 7. The summation was performed over a 20-keV window centered on the 190-keV photopeak of Kr-81m. The observed Kr-81m count rates were normalized to the 511-keV photopeak of Rb-81 in order to correct for changes in geometry due to bubbling in the phantom.

In order to simulate the range of scatter and attenuation encountered in clinical applications, measurements were made with only the inherent attenuation of the phantom ($\simeq 2$ cm) and were repeated with 5 cm of added tissue-equivalent material.

RESULTS

Figure 5 shows a comparison of the results obtained with the contaminated commercial samples and with the pure cyclotron-produced samples. Each data point represents the mean ± S.E.M. of the observed ratio ($R = C_2^\circ/C_2$) of Kr-81m count rates at that flow rate. A slightly higher ratio, and therefore a higher estimate of flow, was obtained with the commercial samples. The linear regression line for Fig. 5 is

$$R_p = (0.98 \pm 0.01)\ R_c + (0.006 \pm 0.015),$$
$$r = 0.999,$$

where R_p and R_c are the observed ratios for the pure and commercial samples, respectively. The quoted uncertainties are one standard deviation, and r is the correlation coefficient. The mean flow measured with the commercial samples was 8% higher than with the pure samples at a fl^w comparable to 122 cc/min per 100 gm, and was 4% higher at 232 cc/min per 100 gm. This small difference between the results obtained with the pure and commercial samples is probably due to differences in the Compton distribution and corresponding errors in the Compton correction based on a linear extrapolation.

Figure 6 shows the observed ratio ($R = C_2^\circ/C_2$) as a function of the flow-rate constant (k_f) calibrated with Xe-133. Because the differences in ratios obtained with pure and commercial Rb-81 were small, the results from the pure and commercial samples have been combined to give a single mean ± S.E.M. at each flow value. The straight line is the theoretical response

$$R = (18.76\ \text{sec})\ (k_f\ \text{sec}^{-1}) + 1.0$$

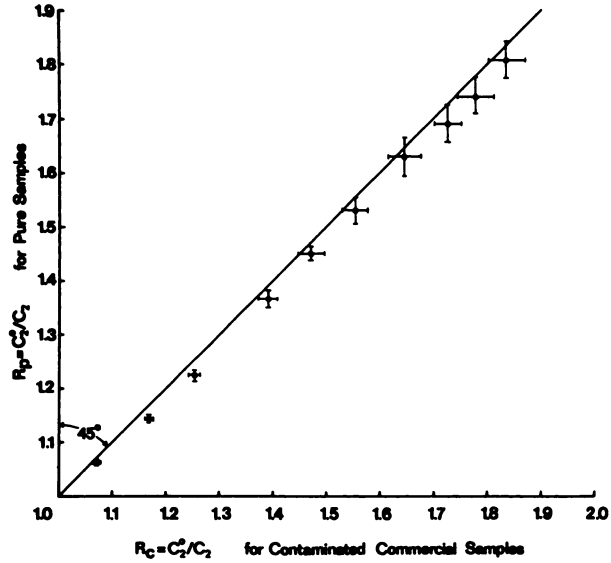predicted by Eq. 6. Results are shown for both tissue

FIG. 5. Comparison of ratios of Kr-81m count rates measured with pure (R_p) and contaminated (R_c) samples. Each point represents mean ± S.E.M. of observed ratios at preselected flow rate.
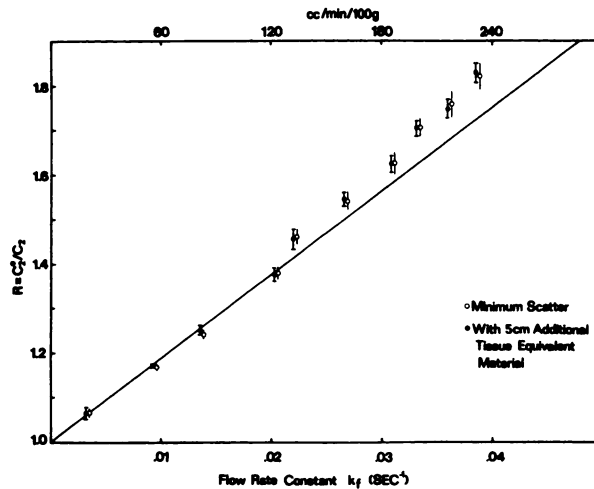

FIG. 6. Observed ratio of Kr-81m count rate in absence of flow (C_2°) to that with flow (C_2), as function of calibrated flow rate constant (k_f). Each point is mean ± S.E.M. Straight line is theoretical response predicted by Eq. 6.

depths investigated. In each case the agreement for rate constants up to 0.02 sec^{-1} is excellent, with a linear regression for the first four points of

$$R = (18.5 \pm 0.7\ \text{sec})\ (k_f\ \text{sec}^{-1})$$
$$+ (1.000 \pm 0.009), r = 0.998,$$

in the minimum scatter case, and

$$R = (18.3 \pm 0.3\ \text{sec})\ (k_f\ \text{sec}^{-1})$$
$$+ (1.003 \pm 0.004), r = 0.999,$$

when 5 cm of tissue-equivalent material was added. At the higher flow rates the observed ratio deviates systematically from the predicted linear response. The largest ratio (R = 1.825) was observed with minimum scatter at a rate constant 12% smaller than predicted by theory. At maximum flow, the magnitude of the Compton correction ranged from 18% of the total counts in the 190-keV window with a pure sample and minimum scatter, to 57% with a contaminated sample and maximum scatter.

DISCUSSION

At present, the inert-gas washout technique provides the only available method for quantifying regional myocardial blood flow in man. When Xe-133 is used as the radiotracer, there are a number of inherent limitations to the technique. Xenon is more soluble in fat than in myocardial tissue or blood. As a result, washout of xenon from adipose tissues is only about one-tenth as rapid as from myocardial tissues with the same blood flow. This probably results in some underestimation of blood flow to the myocardium, and when repeated studies are performed, radioxenon within adipose tissues causes substantial background radioactivity.

Another disadvantage of the radioxenon technique is that repeat studies necessitate the recatheterization of the artery feeding the organ of interest, since re-injection of Xe-133 is necessary for each measurement. Thus, the entire study must be performed in the angiographic suite, and methods for enhancing blood flow are limited to those mechanical and pharmacologic interventions that can be introduced with the patient lying on the angiographic table (21,22).

Initial attempts to use the ^{81}Rb–^{81m}Kr system for the measurement of blood flow have demonstrated that flow measurements are possible only in organ systems with high flow rates because of the short physical half-life of Kr-81m. Furthermore, the brain is not a suitable organ for this approach because the transport of potassium analogues across the blood-brain barrier is exceedingly slow. This limits the technique to organs with relatively high flow rates, such as the myocardium, kidneys, and spleen. Attempts to measure myocardial blood flow following an intravenous injection of Rb-81 have been hampered by a number of problems. First of all, rubidium is also deposited in overlying structures. Secondly, krypton returning to the right side of the heart from the rest of the body (particularly the kidneys) makes accurate estimates of the Kr-81m count rate extremely difficult. Finally, determination of the depth of the myocardium within the body, in order to correct to tissue attenuation, is difficult.

An alternative approach would be the direct injection of Rb-81 into the artery supplying the organ of interest. Measurements could begin within one minute of the injection of Rb-81, since the Kr-81m count rate (C_2) approaches its equilibrium value at a rate determined by k_{eff}. In the case of the heart, the extraction fraction during a single pass of rubidium is 65% (23); consequently, the great bulk of the radiorubidium would be within the myocardium. Since the distribution of the rubidium would be proportional to blood flow, there would not be a disproportionate accumulation of the radiotracer within pericardial fat. Furthermore, repeat injections would not be necessary since the radioactive inert gas would continue to be produced as long as the parent remained in the myocardium. Since the half-time for the washout of rubidium from the myocardium is greater than one hour, it would be anticipated that adequate time would be available for estimation of flow under several physiologic conditions following a single intra-arterial injection.

This study suggests that ^{81}Rb–^{81m}Kr can be used to measure regional blood flow in vivo with currently available NaI detecting systems after the injection of Rb-81 into the arterial systems supplying the organ of interest. The simple crossover correction used here was adequate for a wide variety of sample purities and scattering conditions. While it has been suggested that pure Rb-81 is required for accurate assessment of flow (5), the ratios measured with the commercial samples contaminated with Rb-82m were only slightly higher than those measured with the pure samples. This is because the measurement is based not on the ratio of Kr-81m to Rb-81, but rather on flow-dependent changes in the Kr-81m count rate from its value in the absence of flow. Thus, the true Rb-81 count rate is not needed to measure the flow accurately.

The advantages of pure ^{81}Rb–^{81m}Kr are, then, relatively minor. The Compton correction is smaller for a pure sample, and the unnecessary patient dose due to contaminating isotopes is eliminated. Furthermore, the normalization of the Kr-81m count rate to eliminate geometric effects drifts slowly with time for a contaminated sample, due to the slow buildup of Rb-82m. If Rb-82m contributes 30% of the counts in the 511-keV photopeak (as is the case in Fig. 2B), the normalization will drift by only $\approx 1\%$ per hour. Thus, if the measurements with and without flow are made in rapid succession, this problem becomes negligible. The advantages of a pure sample must be weighed against the convenience and availability of commercially produced Rb-81.

The most serious problem in the clinical application of this technique is the simulation of the zero-flow spectrum. The measured flow rate is extremely

sensitive to errors in the zero-flow count rate (C_2^o). For example, an estimate of C_2^o that is 10% too high will result in an erroneous overestimation of flow of 42% when the true flow is 100 cc/min per 100 gm. For in vivo studies, the zero-flow measurement could be obtained after injecting Rb-81 into the balloon of a Swann-Gans catheter placed within the left ventricle.

Another apparent problem is the overestimation of flow at high flow rates. Since the deviation from the predicted response was comparable over a wide range of Compton corrections, it is not believed that this deviation is due entirely to an overestimation of the Compton crossover, although such an error would become increasingly important at high flow rates and may be a contributing factor.

A more likely explanation of the deviation at high flow rates is the difference in diffusivities between the Xe-133 used to calibrate the phantom and the Kr-81m used in the actual measurements. The response at high flow rates suggests that the washout of Kr-81m may be less limited by diffusion than is that of Xe-133. This result is expected (24) on the basis of the smaller molecular radius of Kr-81m, and is, of course, an advantage in clinical applications.

The deviation from linearity seen in Fig. 6 must then be interpreted as an upper limit to the inherent inaccuracy of the technique when a simple linear extrapolation is used to correct for the Compton crossover. Both the accuracy and precision of the flow measurements are adequate for most clinical applications.

For regional flow measurements with an Anger camera, complete energy spectra from each region will not be available. Flow measurements may, however, be based on the count rates in two windows, one centered on the 190-keV Kr-81m peak and another on the Compton continuum. The count rate of the Compton continuum (window 2) would be used both to normalize the Kr-81m count rate (window 1) for geometry and to estimate the Compton contribution in the Kr-81m window. A single complete energy spectrum could provide the ratio of the Compton counts in window 2 to those in window 1, based on the linear extrapolation used in this study.

FOOTNOTES

* Medi-Physics, Inc., Emeryville, Calif.

† Gilmont 3235, Gilmont Instruments, Great Neck, N.Y.

REFERENCES

1. CANNON PJ, DELL RB, DWYER EM: Measurement of regional myocardial perfusion in man with ^{133}Xenon and a scintillation camera. *J Clin Invest* 51: 964–977, 1972

2. HOLMAN BL, ADAMS DF, JEWITT D, et al.: Measuring regional myocardial blood flow with ^{133}Xe and the Anger camera. *Radiology* 112: 99–107, 1974

3. JONES T, MATTHEWS CME: Tissue perfusion measured using the ratio of ^{81}Rb to ^{81m}Kr incorporated in the tissue. *Nature* 230: 119–120, 1971

4. JONES T, PETTIT JE, RHODES CG, et al.: Use of ^{81}Rb–^{81m}Kr ratio for measurement of spleen blood flow. *J Nucl Med* 14: 414, 1973

5. HARPER PV, RICH B, LATHROP KA, et al.: Production and use of ^{81}Rb–^{81m}Kr for clinical tissue perfusion measurements with the Anger camera. In *Dynamic Studies with Radioisotopes in Medicine, 1974*, Vienna, IAEA, vol. 2: 133–143, 1975

6. KAPLAN E, MAYRON LW, FRIEDMAN AM, et al.: Definition of myocardial perfusion by continuous infusion of krypton-81m. *Am J Cardiol* 37: 878–884, 1976

7. KAPLAN E, MAYRON LW: Evaluation of perfusion with the ^{81}Rb–^{81m}Kr generator. *Sem Nucl Med* 6: 163–192, 1976

8. TURNER JH, SELWYN AP, CLARK JC, et al.: Continuous measurement and imaging of regional myocardial perfusion using krypton-81m. *J Nucl Med* 17: 535–536, 1976

9. JONES T, CLARK JC, HUGHES JM, et al.: ^{81m}Kr generator and its uses in cardiopulmonary studies with the scintillation camera. *J Nucl Med* 11: 118–124, 1970

10. YANO Y, McRAE J, ANGER HO: Lung function studies using short-lived ^{81m}Kr and the scintillation camera. *J Nucl Med* 11: 674–679, 1970

11. DILLMAN LT, VON DER LAGE FC: *Radionuclide Decay Schemes and Nuclear Parameters for Use in Radiation-Dose Estimation. MIRD Pamphlet No 10*, New York, Society of Nuclear Medicine, 1975, p 52, 54

12. BRODA R, HRYNKIEWICZ AZ, STYCZEN J, et al.: The excited states of krypton and rubidium isotopes in the $78 \leq A \leq 85$ mass region. *Nucl Phys* A216: 493–518, 1973

13. WATERS SL, SILVESTER DJ, GOODIER IW: Decay of ^{81}Rb. *Phys Rev C* 2: 2441–2443, 1970

14. HOLMAN BL, ELDH P, ADAMS DF, et al.: Evaluation of myocardial perfusion after intracoronary injection of radiopotassium. *J Nucl Med* 14: 274–278, 1973

15. SCHNEIDER RJ, GOLDBERG CJ: Production of rubidium-81 by the reaction ^{85}Rb(p,5n)^{81}Sr and decay of ^{81}Sr to ^{81}Rb. *Int J Appl Radiat Isot* 27: 189–191, 1976

16. KOPECKY P, MUDROVA B: The separation of carrier-free ^{85}Sr from a cyclotron target. *Int J Appl Radiat Isot* 25: 469–470, 1974

17. HARDEWIG A, ROCHESTER DF, BRISCOE WA: Measurement of solubility coefficients of krypton in water, plasma and human blood, using radioactive Kr^{85}. *J Appl Physiol* 15: 723–725, 1960

18. MORRISON TJ, JOHNSTONE NB: Solubilities of the inert gases in water. *J Chem Soc* 3: 3441–3446, 1954

19. LAWRENCE JH, LOOMIS WF, TOBIAS CA, et al.: Preliminary observations on the narcotic effect of xenon with a review of values for solubilities of gases in water and oils. *J Physiol* 105: 197–204, 1946

20. HERD JA, HOLLENBERG M, THORNBURN GD, et al: Myocardial blood flow determined with krypton-85 in unanesthetized dogs. *Am J Physiol* 203: 122–124, 1962

21. HOLMAN BL, COHN PF, ADAMS DF, et al.: Regional

myocardial blood flow during hyperemia induced by contrast agent in patients with coronary artery disease. *Am J Cardiol* 38: 416–421, 1976

22. JEWITT D, HOLMAN BL, ADAMS DF, et al.: Measurement of regional myocardial blood flow in coronary artery disease. *Brit Heart J* 35: 863, 1973

23. LOVE WD, ISHIHARA Y, LYON LD, et al.: Differences in the relationships between coronary blood flow and myocardial clearance of isotopes of potassium, rubidium and cesium. *Am Heart J* 76: 353–355, 1968

24. KAMAL MR, CANJAR LN: Diffusion coefficients. *Chem Eng Prog* 62: 82–86, 1966

2nd ANNUAL WESTERN REGIONAL MEETING

THE SOCIETY OF NUCLEAR MEDICINE

October 21–23, 1977   **Aladdin Hotel**   **Las Vegas, Nevada**

SIXTH ANNOUNCEMENT AND CALL FOR ABSTRACTS FOR SCIENTIFIC PROGRAM

The Scientific Program Committee welcomes the submission of abstracts of original contributions in nuclear medicine from members and nonmembers of the Society of Nuclear Medicine for the 2nd Annual Western Regional Meeting. Physicians, Scientists, and Technologists, members and nonmembers are invited to participate. The Program will be structured to permit the presentation of papers from all areas of interest in the specialty of Nuclear Medicine. A separate set of guidelines will be used to judge the Technologist abstracts. Abstracts for the scientific program will be printed in the program booklet and will be available to all registrants at the meeting.

GUIDELINES FOR SUBMITTING ABSTRACTS

The abstracts will be printed from camera-ready copy provided by the authors. Therefore, only abstracts prepared on the official abstract form will be considered. These abstract forms will be available from the Western Regional Chapter's SNM office (listed below). Abstract forms will only be sent to SNM members of the Pacific Northwest, Southern California, Northern California, and Hawaii Chapters in a regular mailing. All other requests will be sent on an individual basis.

All participants will be required to register and pay the appropriate fee.

Please send the original abstract form, supporting data, and six copies to:

> Jean Lynch, Administrative Coordinator
> 2nd Western Regional Meeting
> P.O. Box 40279
> San Francisco, CA 94140

Deadline for abstract submission: Postmark midnight, July 8, 1977.